PHYSICAL REVIEW E **78**, 020401(R) (2008)

Static structure of confined dumbbell-sphere colloidal mixtures

Andrés García-Castillo and José Luis Arauz-Lara
Instituto de Física "Manuel Sandoval Vallarta," Universidad Autónoma de San Luis Potosí, Alvaro Obregón 64, 78000 San Luis Potosí, S.L.P., Mexico

(Received 23 May 2008; published 6 August 2008)

The static structure of quasi-two-dimensional colloidal mixtures of dumbbells and spheres is studied by optical microscopy. Colloidal dumbbells, produced by aggregation of colloidal spheres, are mixed with spherical particles and confined between two parallel glass walls. The static structural properties of this system are determined for various concentrations of spheres in the dilute limit of dumbbells. The dumbbell-sphere pair correlation function exhibits a strong angular dependence, and also shows that the presence of dumbbells favors the formation of triangular lattices even at sphere concentrations far from close packing.

DOI: 10.1103/PhysRevE.78.020401 PACS number(s): 82.70.Dd, 05.40.−a

The structural properties of confined colloidal suspensions are of current interest and are studied experimentally, under different conditions, by optical microscopy [1–9]. Particularly, the interest has been focused in monodisperse quasi-two-dimensional (Q2D) systems, where a suspension of spherical colloidal particles of uniform size (in the micrometer range) is confined between two parallel plane plates separated at a distance slightly larger than the particles' size. Under such conditions, the particles form a single layer between the plates and one can use optical methods to image local (within the field of view) equilibrium configurations of the system at different times. From the analysis of such configurations it has been possible to determine physical quantities such as the static and dynamic structures arising from the interparticle correlations [2–4,10–15]. In a homogeneous monodisperse system of spherical particles, the static structure is described by the pair correlation function $g(\mathbf{r}_1,\mathbf{r}_2)$, which is the conditional probability of finding a particle at the position $\mathbf{r}_2$ given that one particle is at $\mathbf{r}_1$. When the interparticle interactions are spherically symmetric, the pair correlation function depends only on the interparticle distance $r=|\mathbf{r}_2-\mathbf{r}_1|$, i.e., $g(\mathbf{r}_1,\mathbf{r}_2)\equiv g(r)$ where $g(r)$ is referred to as the radial distribution function and describes the equilibrium average distribution of the colloidal particles around one of them. However, in nature and in many synthetic materials, colloidal species are not always spherical particles in the unbounded homogeneous three-dimensional space. For instance, proteins embedded in a biological cell membrane are nonspherical particles constrained to move in a two-dimensional (2D) space, hydrocarbon aggregates in oil fields are frequently buried in porous and fractured rocks, etc. Thus, it is important to investigate the structural properties of nonspherical particles in confined geometries. Here we consider the case of dumbbell particles in a monodisperse suspension of spheres confined in a Q2D geometry. We use optical microscopy to measure the local structure of the spherical particles around the dumbbells in the dilute limit of the latter, such that no phase separation is observed [16]. As we see below, the nonspherical shape of the dumbbells induces an angular dependence of the dumbbell-sphere pair correlation function. Figure 1 shows illustrative images of the system of interest. In Fig. 1(a) it shows an image of a Q2D colloidal suspension containing dumbbell particles in a sea of monodisperse spheres at the area fraction of spheres $\phi_a=0.54$. The spheres are polystyrene particles of diameter $\sigma=1.9$ μm and the dumbbells are formed by two of those spheres, irreversibly stuck to each other. In this static picture, the dumbbells are encircled to distinguish them from those pairs formed momentarily. Figures 1(b)–1(k) show images taken at time intervals of 5 s of a small region of the system, at the center part of Fig. 1(a), containing a single dumbbell surrounded by spheres. This sequence allows one to appreciate the time scale of the changes in the positional and orientational configuration of the dumbbells and the time evolution of the local configuration of spheres.

The preparation of quasi-two-dimensional colloidal mixtures of dumbbells and spheres is done as follows. Protocols for the fabrication of dumbbells from uniform spheres are available in the literature [17–19]; here we follow the aggregation and fractionation procedure described below. A monodisperse water suspension of polystyrene spheres of diameter σ, carrying negatively charged sulfate end groups on the sur-

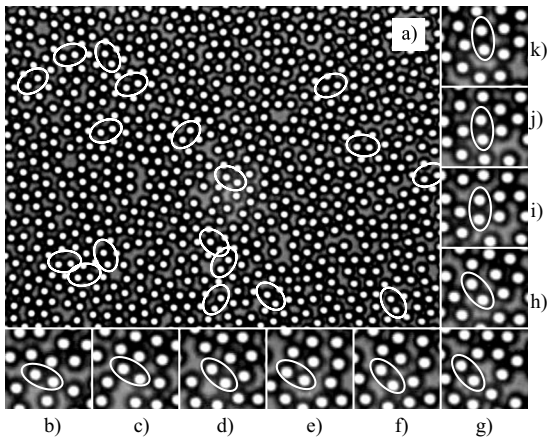

FIG. 1. (a) Optical microscopy image of dumbbell particles (encircled) in a monodisperse suspension of spheres. The spherical particles are polystyrene particles of diameter $\sigma=1.9$ μm and the dumbbells are formed by two of those spheres irreversibley stuck together. The suspension is confined between two glass plates separated at a distance $h=3.0$ μm, forming in this way a quasi-two-dimensional colloidal suspension. Figures 1(b)–1(k) are enlarged images of a small squared box at the center of (a), containing individual spheres and only one dumbbell. These pictures were taken at time intervals of 5 s.

face, is extensively dialyzed against ultrapure water to eliminate the surfactant added by the manufacturer (Duke Scientific). In a portion of the clean suspension, particle aggregation is promoted by the addition of NaCl in a sufficient amount to reach a final salt concentration of 500 mM. This process is quenched after five minutes by dialysis of the system in clean water. The suspension (contained in a closed vial immersed in glycerol) is then heated up to a temperature of 104 °C (which is above the polystyrene glass transition temperature) for 20 min to produce sintering of particles in contact. The suspension is allowed to cool down to room temperature, then the different aggregates formed are separated by centrifugation in a sugar density gradient tube. The dimers band is recovered from the tube, and the particles are resuspended in clean water and dialyzed again to eliminate the sugar. The clean suspension of dimers is mixed with spherical particles at different proportions. The mixture is then confined between two glass plates following a standard procedure [12]. Briefly, in a clean atmosphere of nitrogen gas, the mixture of spheres and dumbbells is mixed with a small amount of larger particles of diameter h. A small volume of this mixture ($\approx 1\ \mu$l), is confined between two clean glass plates (a slide and a cover slip), which are uniformly pressed one against the other until the separation between the plates is h. Thus, the larger particles scattered across the sample serve as spacers with an average distance of $\sim 100\ \mu$m between them. The system is then sealed with epoxy resin, and both species of mobile particles are allowed to equilibrate in this confined geometry at room temperature (24 ± 0.1 °C). The particles and the glass plates are negatively charged and they repel each other. However, although we do not add any electrolyte, the solution has a high ionic strength due to the ionic species dissociated from the glass walls [1]. Thus, the electrostatic repulsion is screened and the particles can approach each other and eventually aggregate or stick to the walls. Then, in order to help prevention against aggregation we added SDS [sodium dodecyl sulfate, enough to reach the critical micelar concentration (CMC)] to the mixture of colloidal particles.

The samples are observed from a top view (perpendicular to the walls plane), using an optical microscope with a 60 × objective of numerical aperture 1.0. The motion of the particles is recorded using standard video equipment. The field of view is $\sim 80 \times 60\ \mu\text{m}^2$ (640×480 pixels). Since $h/\sigma \approx 1.6$, the motion of the particles perpendicular to the walls is highly restricted and the systems are treated as effectively two dimensional. Images of each system considered here, are digitized and analyzed to obtain the x and y coordinates of the spherical particles and those of the center of mass of the dumbbells, and the orientations of the latter. From that data, we determine the dumbbell-sphere and sphere-sphere pair correlation functions from each image and the final results presented below are the average over the total video frames analyzed. Since the dumbbell-sphere correlation function depends on both spatial and angular variables, we need to analyze a very large number of particle configurations to accurately determine such dependence. In practice, the pair correlation function is determined only in discrete values of θ and r, defined in Fig. 2, by counting all the particles within the neighborhood $(r \pm \Delta r, \theta \pm \Delta\theta)$. Here

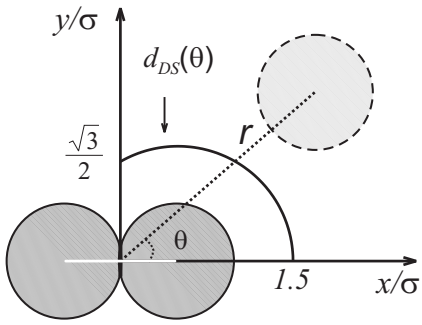

FIG. 2. Schematic of the geometry dumbbell sphere. The two gray circles represent a dumbbell with its long axis along the x direction. The center of coordinates is placed at the dumbbell's center of mass. The dashed circle represents a single sphere located at a distance r and angle θ. The solid line represents the angle depending distance of closest approach of a hard disk to a hard dumbbell $d_{DS}(\theta)$, given in Eq. (1).

we take $\Delta r = 0.05\sigma$ and $\Delta\theta = 5°$. Thus, in order to ensure statistical independence of particle configurations and smooth correlation functions, we analyzed a number of video frames in the order of 2×10^5, corresponding to 2 h of continuous recording of the system's evolution, at a rate of 30 frames/s. Since the correlation time of the particle configurations is in the order of few seconds [13], the total recording time spans over three decades of that correlation time. An impression of the system's time-scale evolution can be obtained from Figs. 1(b)–1(k). Actual dumbbells are distinguished from those formed momentarily by following the trajectories of all particles in the field of view during the total time of the experiment.

Our results are presented in Figs. 3–5. Figure 3 shows the pair correlation functions (a) sphere-sphere $g_{SS}(r)$ and (b) dumbbell-sphere $g_{DS}(r,\theta)$ in a system where $\sigma = 1.9\ \mu$m, $h = 3.0\ \mu$m, and $\phi_a = 0.54$. As one can see in Fig. 3(a), at this area fraction the sphere-sphere correlation function (closed circles) has a high first maximum near to contact followed by other oscillations of short range in accordance with a system of particles with an effective short ranged interaction in the liquid state. In Fig. 3(b) each curve represents $g_{DS}(r,\theta)$ as a function of r for a fixed value of θ. We present here the results for θ in the range of 0°–90°, in steps of 5°. Let us note that due to the symmetry of the dumbbell (see Fig. 2), we need to consider only the first quadrant. The curves in the other quadrants are mirror images of those in the first quadrant and they are averaged together to increase the statistics. Thus, as one can see here, various features of the dumbbell-sphere correlation function differ notably from those of the sphere-sphere correlation function. First of all, one can note a strong and complex angular dependence of the pair correlation function $g_{DS}(r,\theta)$. At low values of θ (i.e., $\sim 0°$) the dumbbell-sphere correlation function is practically the correlation function between spheres $g_{SS}(r)$. This can be seen in Fig. 3(a) where $g_{DS}(r-\sigma/2, \theta = 0°)$ is shown for comparison with the sphere-sphere correlation function. This means that the spherical particles being along the long axis of the dumbbell regard it as an individual sphere, i.e., the partner particle at the other side has no influence on the correlation function

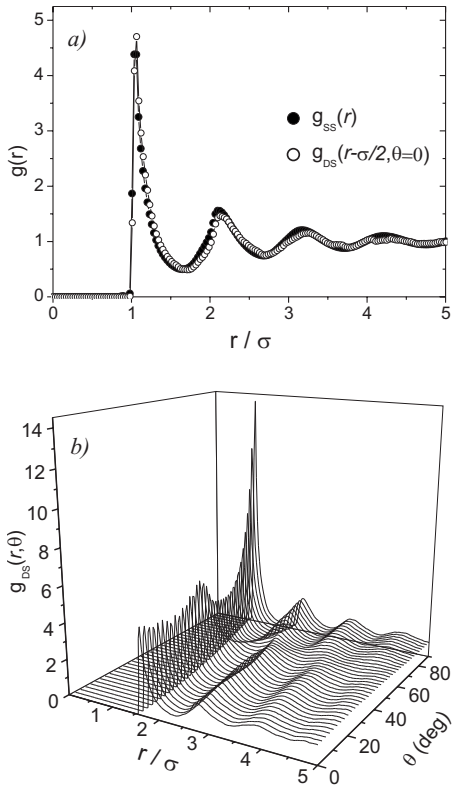

FIG. 3. (a) Sphere-sphere pair correlation function (closed circles) in a system with $\phi_a=0.54$. For comparison, the dumbbell-sphere correlation function $g_{DS}(r-\sigma/2,\theta=0°)$ is also presented (open circles) (see the text for discussion). (b) Dumbbell-sphere correlation function $g_{DS}(r,\theta)$ vs r for values of θ in the range of 0°–90°, in steps of 5° (solid lines).

at this value of θ. On the other hand, for $\theta>0$ the presence of the second particle forming the dimer produces a strong angular dependence on $g_{DS}(r,\theta)$. The most notable effects are the nonmonotonic dependence of the height of the first peak $g_{max}(\theta)$ and the shift in the position of the first maximum $r_{max}(\theta)$. The former can be appreciated better in Fig. 4 where $g_{max}(\theta)$ vs θ is shown for different values of the area

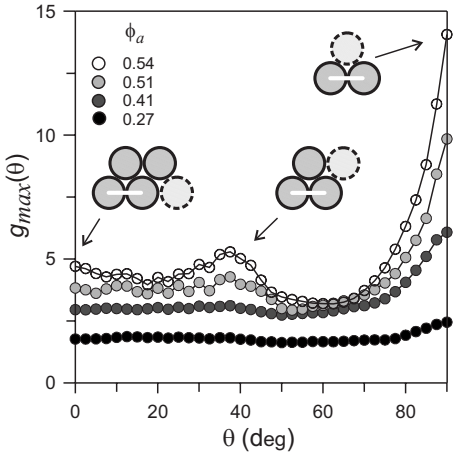

FIG. 4. The height of the first peak of the dumbbell-sphere correlation function vs θ for different concentrations of spheres (symbols). The solid lines are guides to the eye.

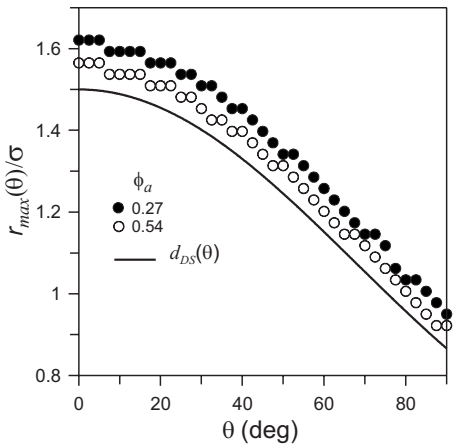

FIG. 5. Position of the first peak of the dumbbell-sphere correlation function as a function of θ for $\phi_a=0.27$ (closed circles) and 0.54 (open circles). The solid line is the distance of closest approach of a hard disk to a hard dumbbell $d_{DS}(\theta)$.

fraction of spheres ϕ_a (symbols). Here one can see that for $\phi_a \lesssim 0.41$ the height of the first peak has little dependence on θ in the range 0°–75°, and at larger angles it starts to increase monotonically reaching its maximum at $\theta=90°$. At higher particle area fractions, $g_{max}(\theta)$ has a more interesting behavior. For instance, at $\phi_a=0.54$ the height of the first peak initially decreases with θ, then it increases reaching a local maximum at around $\theta=40°$, it then decreases having a local minimum at $\theta\sim 60°$, and finally, it increases again reaching its maximum at $\theta=90°$. Thus, the probability of finding a spherical particle close to the dumbbell is highest at $\theta=90°$, i.e., in the region between the two particles forming the dumbbell, and this probability increases with ϕ_a. This means that, as the concentration of particles increases, the most likely dumbbell-sphere configuration is the triangular one, which is the close packing configuration of spheres in a 2D crystal. In the case of a 2D crystal, a sphere sitting in the interstitial area between two spheres (i.e., at $\theta=90°$) would produce an exclusion zone to other neighbor particles from being at angles $\theta<40°$, and the next particle would have its highest probability at $\theta\sim 40°$. This fourth sphere would in turn exclude neighbor particles except at around $\theta=0°$. Interestingly, the maxima and minima of $g_{max}(\theta)$ are located at the same angular positions of a 2D crystalline structure, although in our case the peaks are not sharp because our systems are still in the liquid phase. Thus, our measurements of $g_{max}(\theta)$ show that at high particle concentrations, but still far from the close packing concentration of particles $\phi_a\sim 0.91$, our system already exhibits an incipient crystalline structuring of spheres around single dumbbells.

Figure 5 shows the position of the first maximum $r_{max}(\theta)$, as a function of the angle, measured in two of the systems considered in Fig. 4: $\phi_a=0.27$ (closed circles) and $\phi_a=0.54$ (open circles). As one can see here, $r_{max}(\theta)$ decreases as the angle increases and the trend is quite similar for both concentrations of particles; in fact one curve can be obtained from the other by a small shift in the vertical direction (the curves for the other values of ϕ_a considered here follow the same trend and fall in between the curves in Fig. 5). In Fig.

5 we compare our results with the calculated angle dependent distance of closest approach $d_{DS}(\theta)$, of a hard disk to a dumbbell formed by two hard disks of the same diameter, given by Eq. (1) (solid line). As one can also see here, the measured position of the first peak coincides qualitatively very well with $d_{DS}(\theta)$ and the quantitative agreement is better as the particle concentration increases.

$$d_{DS}(\theta) = \frac{\sigma}{2}[\cos(\theta) + \sqrt{3 + \cos^2(\theta)}]. \quad (1)$$

In this work we address the issue of the static structure of a confined binary mixture of colloidal particles consisting of dumbbells and spheres in the dilute limit of the former. The particles are dispersed in water and restricted to move between two parallel plates becoming in this way an effective two-dimensional system. The analysis of the local structure of spheres around a single dumbbell shows a strong angular dependence of the dumbbell-sphere pair correlation function, being more pronounced for more concentrated systems (Fig. 3). As it is shown in Fig. 4, at high concentrations of spheres the presence of dumbbells induces the formation of local crystalline structures. This arises the question of whether few dumbbell impurities present in a monodisperse suspension of effective hard spheres would produce any appreciable effect on the order-disorder transition of the system. Our results suggest they would, but considerably more experimental and theoretical work is needed to get a definite answer.

We acknowledge technical support from A. Ramírez-Saito, and financial support from Consejo Nacional de Ciencia y Tecnología, México, and from Fondo de Apoyo a la Investigación (FAI-UASLP).

[1] C. A. Murray and D. G. Grier, Annu. Rev. Phys. Chem. **47**, 421 (1996).
[2] G. M. Kepler and S. Fraden, Phys. Rev. Lett. **73**, 356 (1994).
[3] M. D. Carbajal-Tinoco, F. Castro-Román, and J. L. Arauz-Lara, Phys. Rev. E **53**, 3745 (1996).
[4] S. H. Behrens and D. G. Grier, Phys. Rev. E **64**, 050401(R) (2001).
[5] D. T. Wasan and A. D. Nikolov, Nature (London) **423**, 156 (2003).
[6] K. Zahn, A. Wille, G. Maret, S. Sengupta, and P. Nielaba, Phys. Rev. Lett. **90**, 155506 (2003).
[7] P. N. Pusey, Science **309**, 1198 (2005).
[8] K. Kang, J. Gapinski, M. P. Lettinga, J. Buitenhuis, G. Meier, M. Ratajczyk, J. K. G. Dhont, and A. Patkowski, J. Chem. Phys. **122**, 044905 (2005).
[9] C.-Y. Chou, B. C. Eng, and M. Robert, J. Chem. Phys. **124**, 044902 (2006).
[10] J. Baumgartl and C. Bechinger, Europhys. Lett. **71**, 487 (2005).
[11] B. Cui, B. Lin, S. Sharma, and S. A. Rice, J. Chem. Phys. **116**, 3119 (2002).
[12] A. Ramírez-Saito, M. Chávez-Páez, J. Santana-Solano, and J. L. Arauz-Lara, Phys. Rev. E **67**, 050403(R) (2003).
[13] J. Santana-Solano and J. L. Arauz-Lara, Phys. Rev. Lett. **87**, 038302 (2001).
[14] B. Cui, H. Diamant, B. Lin, and S. A. Rice, Phys. Rev. Lett. **92**, 258301 (2004).
[15] J. Santana-Solano, A. Ramírez-Saito, and J. L. Arauz-Lara, Phys. Rev. Lett. **95**, 198301 (2005).
[16] Z. Dogic, D. Frenkel, and S. Fraden, Phys. Rev. E **62**, 3925 (2000).
[17] P. M. Johnson, C. M. van Kats, and A. van Blaaderen, Langmuir **21**, 11510 (2005).
[18] A. M. Yake, R. A. Panella, C. E. Snyder, and D. Velegol, Langmuir **22**, 9135 (2006).
[19] M. Ibisate, Z. Zou, and Y. Xia, Adv. Funct. Mater. **16**, 1627 (2006).